GEC
GLOBAL ENERGY CONCEPTS
THE Wind Resource

Evaluation of Aeroelastically Tailored Small Wind Turbine Blades Final Project Report

Report # DOE-001

Prepared Under DOE Contract Number
DE-FG36-03GO13133

September 29, 2005

Prepared for:

United States Department of Energy
Golden Field Office
1617 Cole Boulevard
Golden, Colorado 80401

DOE Contacts:
Contract Officer – Beth Dwyer
Project Officer – Keith Bennett
(303) 275-4700

5729 Lakeview Drive NE, Suite 100, Kirkland, Washington 98033
Phone: (425) 822-9008 Fax: (425) 822-9022
www.globalenergyconcepts.com

Table of Contents

List of Figures

List of Tables

Section 1 - Introduction

Global Energy Concepts, LLC (GEC) has performed a conceptual design study to evaluate the potential for aeroelastically tailored rotors designed specifically for small wind turbines. This work has been performed for the U.S. Department of Energy under Grant No. DE-FG36-03GO13133.

1.1 Background

Numerous studies have investigated the cost of energy (COE) reductions that can be achieved via aeroelastically tailored wind turbine blades designed to capture more energy while reducing or mitigating other system loads. The WindPACT Rotor Study predicted an 8.2% reduction in COE that was for a rotor that had the combined features of a slender planform with twist-coupling [1]. The majority of recent work has focused on MW-scale turbines for which aerodynamic forces are dominant, gravity forces are significant, and centripetal loading is negligible. For small wind turbines (SWT) this is not the case. At the lower end of the SWT size range centripetal rotor loads are dominant, followed by aerodynamic loading, with gravity loads being negligible. This not only changes the turbine design challenge, but presents new opportunities for aeroelastically tailored blades.

A report by Zuteck [2] evaluated the potential for swept planforms to affect bend-twist coupling in blades, and showed that substantial coupling could be achieved with modest amounts of sweep. However, because that work was directed primarily toward MW-scale turbines, the work concluded that the feasibility of the concept was questionable due to the cost and complexities associated with curved blade spar structure.

If the blade manufacturing method is changed to injection molding, as is common at the lower end of the small wind turbine size range, the cost penalty for complex shapes can be negligible and the cost-effectiveness of this approach dramatically improved. Because centripetal forces are substantial in small turbine rotors, the inclusion of pre-bending or pre-curving can be used to balance aerodynamic bending moments and offer additional design options for achieving optimal aeroelastic response. This concept forms the basis for the present study.

1.2 Project Overview

The following sections provide a brief overview of the baseline turbine design, project objectives, modeling approach, and matrix of turbine/rotor configurations considered in the study. Each of these topics is then discussed in greater detail in the body of the report.

1.2.1 Baseline Turbine Design

The baseline turbine for this study is based on the Southwest Windpower (SWWP) "AIR-X," which is depicted in Figures 1 and 2. As seen in Figure 2, the AIR-X has a three-bladed, upwind

rotor with a diameter of 1.17 m. The blades are solid plastic (injection-molded). The aerodynamic design incorporates a single airfoil shape, the SD2030.

The earlier SWWP "AIR" designs relied on aeroelastic features (flutter) for overspeed protection in high winds. This caused a loud flutter at wind speeds above 16 m/s.

The AIR-X models introduced a microprocessor-based controller to track peak power at low-to-moderate speeds and to slow the rotor at high wind speeds for overspeed protection. These innovations resulted in increased power performance, improved battery charging capability, greater reliability, and a reduction of the flutter noise relative to the AIR models.

The AIR-X scale of turbine was selected for this study, in collaboration with SWWP, primarily because of its size and blade manufacturing method. The small scale of the rotor dictates that centripetal loading will be dominant, allowing the possibility of achieving the desired aeroelastic response from combined sweep and pre-curve. The blade manufacturing method (injection-molded plastics) presents an opportunity to add this geometric shape complexity with minimal recurring costs.

Although the study has primarily focused on the AIR-X, if an aeroelastically beneficial rotor was developed for this turbine model, the anticipated benefits for the basic AIR designs would be equal to or greater than those for the AIR-X.

Because of the inclusion of blade pre-curve, the exact configuration of the AIR-X turbine could not be used in this study. Specifically, a hypothetical variation of the turbine was developed, which assumed a down-wind, free-yaw architecture. This will be discussed in greater detail in Section 2.0.

Figure 1. AIR-X Turbine from Southwest Windpower

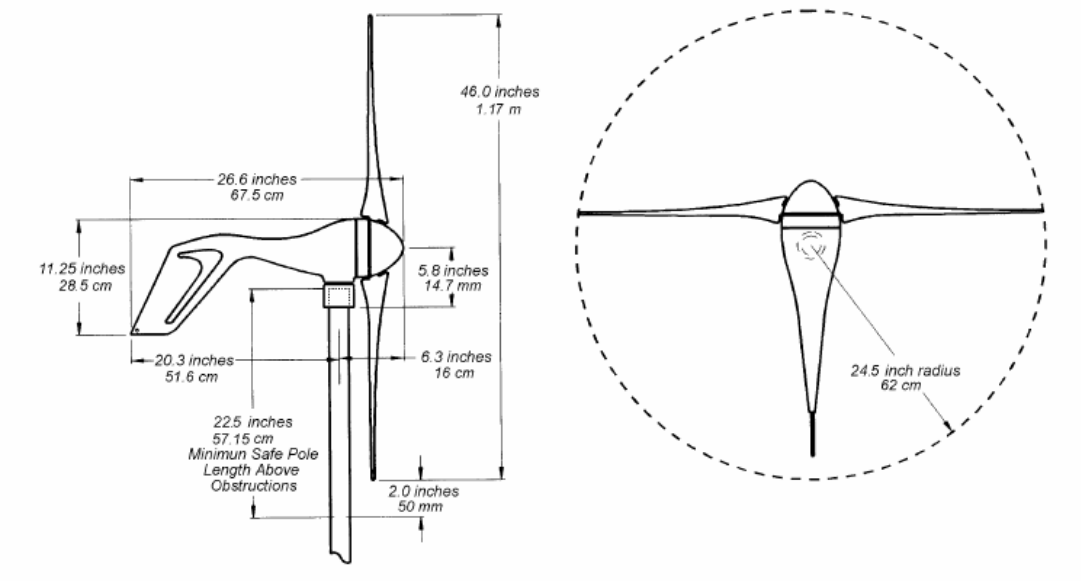

Figure 2. Schematic of AIR-X Turbine

1.2.2 Objectives

This project evaluates ways that blade/rotor geometry could be used in an aeroelastically tailored rotor to enable COE reductions by enhancing energy capture while constraining or mitigating blade costs, system loads, and related component costs. This work builds on insights developed in ongoing adaptive-blade programs but with a focus on application to small turbine systems with isotropic blade material properties and with combined blade sweep and pre-bending/pre-curving to achieve the desired twist coupling. Specific goals of this project are to:

- Evaluate and quantify the extent to which rotor geometry can be used to realize load-mitigating small wind turbine rotors. Primary aspects of the load mitigation are:
  - Improved overspeed safety affected by blades twisting toward stall in response to speed increases.
  - Reduced fatigue loading affected by blade twisting toward feather in response to turbulent gusts.
- Illustrate trade-offs and design sensitivities for this concept.
- Provide the technical basis for small wind turbine manufacturers to evaluate this concept and commercialize if the technology appears favorable.

In addition to these, the original project objectives included the development of an optimized turbine design and evaluation of the potential for load mitigation and COE reductions. As will be detailed in this report, substantial unexpected challenges were encountered in the aeroelastic simulations of these rotors. As a consequence, GEC does not consider the simulation results to be of sufficient confidence to "optimize" a rotor design. Nonetheless, the results of this study provide substantial insights into the design, potential benefits, and challenges (both in practical design and in computational modeling) for this blade technology.

1.2.3 Analysis Tools/Approach

In addition to drawing from all areas of the previous GEC studies concerning blade structural design and aeroelastic tailoring, this study includes substantial new developments in analytical approach and tools. The following list describes the technical areas to be considered and the codes, tools, and technologies to be applied to each:

- Airfoil/Blade Aerodynamic Design
  - NREL airfoil design and testing program
  - PROPID inverse-design code for rotor optimization
  - WT_PERF code for rotor analysis
- Plastic Material Properties
  - Data provided by SWWP
- Blade Structural Design
  - Section properties modeled in SolidWorks
  - Finite Element Analysis (FEA) with the COSMOS code
- Aeroelastic Simulations/Loads Development
  - ADAMS dynamic analysis code with AeroDyn aerodynamics module
  - Wind input for IEC 61400-1 load cases

The baseline blade and turbine system configuration was developed collaboratively with SWWP. The study then focused on making improvements to the baseline design by evaluating further innovations to the blade structural and aerodynamic designs.

Trade-offs were initially performed independently: sweep variations at zero pre-curve (or fixed cone angle), and pre-curve variations at zero sweep. After identifying the basic design sensitivities, structural responses were evaluated for fully coupled designs (sweep + pre-curve).

The ultimate goal of the blade design innovations under consideration is to enable some combination of increased energy capture, reduced aerodynamic loads, and improved safety in overspeed situations The original intent was to use ADAMS simulations both in the basic geometry trade-offs and in the evaluation of aeroelastic response. However, because of the challenges encountered in the ADAMS simulations for these rotor designs, the FEA-based modeling tools provided the primary basis for blade design and evaluation in this project.

Section 2 - Baseline Turbine System Model

As noted above, the baseline used for this study is the AIR-X turbine, modified into a hypothetical downwind, free-yaw configuration. This is shown schematically in Figure 3. In the lower portions on the figure, the side and front views indicate that the blades do not include the features of sweep and pre-curve. With the exception of the root region, the models do include the same chord and twist distributions as the AIR-X blades. Comparing Figures 1 and 3, it can be seen that the baseline GEC configuration has simplified the blade geometry in the root region (approaching the hub). Because this portion of the blade will contribute very little to the loading and aeroelastic response, this simplification was deemed to have negligible effect in the modeling and evaluation of rotor designs.

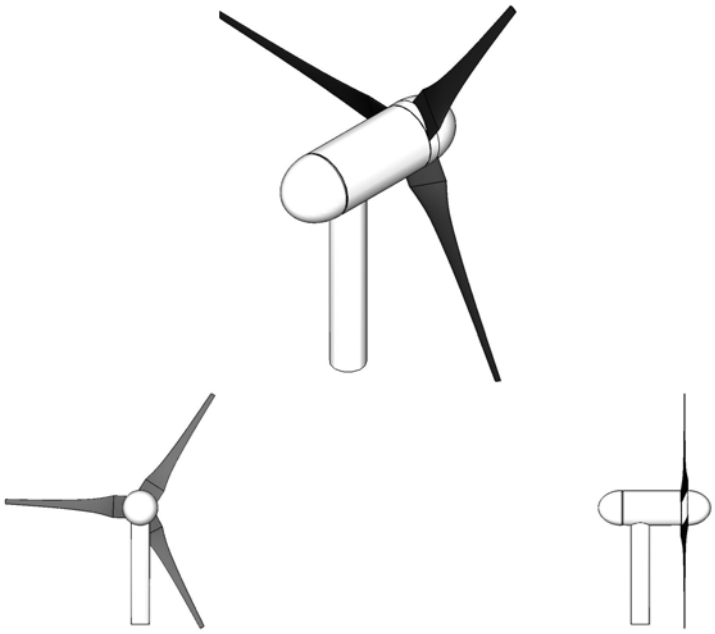

Figure 3. AIR-X Turbine in Hypothetical Downwind Configuration

Section 3 - Aeroelastic Tailoring with Complex Geometry

3.1 Aeroelastic Effects of Sweep and Pre-curve

Figure 4 illustrates the basic features of the rotor geometry under consideration. When compared with a conventional wind turbine blade shape (e.g., as shown in Figure 3), there are two additional types of curvature. The first is a backwards sweeping of the blade planform, and the second is a pre-curve of the blade so that the tip is downwind of the initial plane of rotation. Because of the pre-curve, centripetal forces will create bending moments in the opposite sense of the normal aerodynamic moments. Because of sweep, both the aerodynamic center of pressure and the blade center of mass are aft of the blade root center. As a result, aerodynamic loading (in the positive thrust direction) will cause the blades to pitch towards feather and centripetal loading will cause the blades to pitch toward stall. Stall can be used to affect power regulation, and the aerodynamic twist-coupling to feather will relieve system fatigue loads (blade bending, thrust, tower bending) in response to turbulent gusts.

For the AIR-X and AIR configurations, the most substantial benefits are expected from achieving improved stall characteristic near maximum design rpm. The desired behavior is that an increase in rpm (above a particular design point) will cause the blade to twist towards stall, reducing the rotor thrust, torque, power output, and tendency toward further increases in speed. Such an aeroelastic response would result in additional safety for the AIR-X system and improved stall behavior for the AIR turbines. In either case, these benefits might enable the use of a larger diameter rotor without corresponding increases in tower thrust and/or up-sizing of electrical components for speed control.

At this small turbine scale, reductions of fatigue loads via twist-response to turbulent gusts is expected to be a secondary benefit of the combined sweep and pre-curve. However, this aeroelastic behavior will naturally accompany the speed-twist response for this design concept.

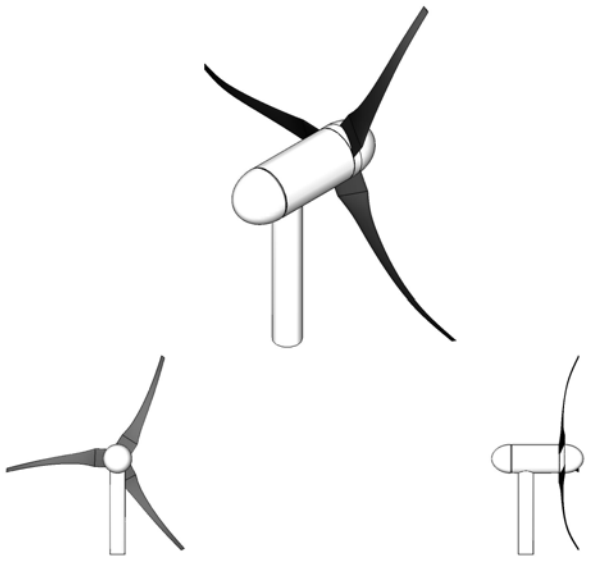

Figure 4. Baseline Rotor with Addition of Blade Sweep and Pre-Curve

3.2 Matrix of Turbine Configurations Evaluated

An extensive matrix of design space for swept/pre-curved blades has been evaluated during this study. Design variables investigated include:

- Aerodynamic design
  - Airfoils
  - Chord and twist distribution
- Sweep
  - Magnitude
  - Shape of sweep distribution
- Pre-curve
  - Magnitude
  - Shape of pre-curve distribution
- Material stiffness and mass density
- Rotor diameter

Changing any of these variables will affect the structural characteristics (mass, bending, and torsional stiffness distributions), the driving loads (centripetal and aerodynamic), and ultimately the aeroelastic response of the rotor.

3.3 Design Points for Aeroelastic Response

Figure 5 shows the approximate relationship between rotor speed and wind speed for the AIR-X turbine. The solid line assumes a tip speed ratio (TSR) of 8.5 up to maximum rotor speed. Figure 5 can be divided into two basic regions of operation. Between wind speeds of 3 and 15 m/s the rotor speed increases steadily with wind speed, with the goal of tracking an optimal blade efficiency and maximizing power output. Above a designated maximum rotor speed (approx. 2000 rpm), some form of speed and/or torque control is required to prevent excessive turbine loads. In the actual AIR-X turbine, active speed control is applied via the alternator to avoid flutter and constrain power and thrust. In the present study, aeroelastic tailoring is evaluated as an alternative approach to controlling rotational speed.

For the purposes of this study, the operating point near 2000 rpm is where a beneficial aeroelastic response is desired. Specifically, the goal is to design a blade such that an increase in rpm will cause sufficient twist (towards stall) so as to achieve self-regulation.

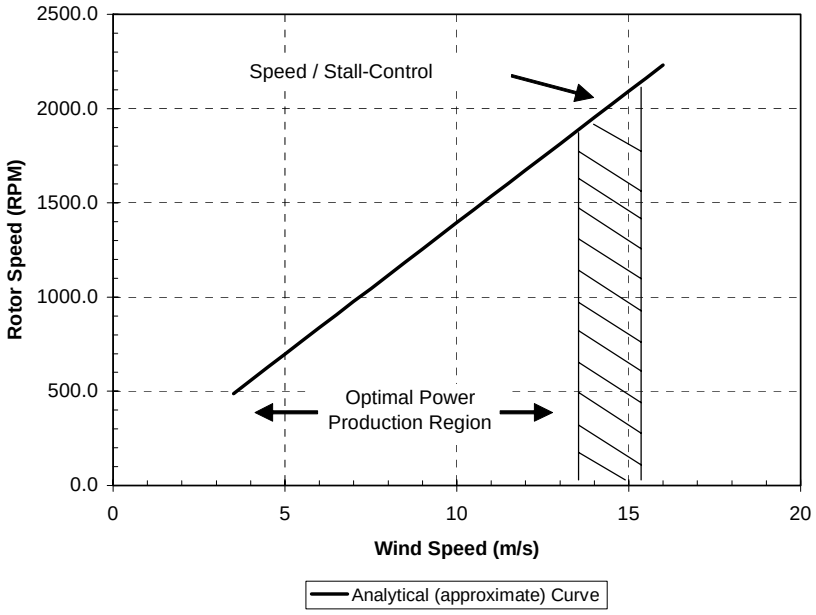

Figure 5. Operating Regions for AIR-X Turbine

At each point in the quasi-steady rotor/wind-speed schedule, there will be an equilibrium balance between the twist (to feather) induced by aerodynamic loads and the twist (towards stall) induced by centripetal loads. In general, it is expected that the blade twist distribution would be changing over the entire range of quasi-steady operating points. Therefore, an optimized version of this rotor concept would involve:

1. Determining a geometry that has an rpm-twist relationship near the maximum rotor speed design point so that the desired self-regulating behavior is achieved.
2. Adjusting the blade twist schedule so that the rotor stays near peak efficiency at wind speeds below maximum rpm.

In embarking on this study, GEC had no assurance that either or both of these design conditions could be met by adding sweep and pre-curve to the AIR-X blade geometry. In conducting the actual project, the major emphasis has been on identifying geometries that show potential for a self-regulating response near maximum rpm. Because of the challenges encountered in achieving this first objective, no attempt was made to re-adjust the blade's twist schedule for optimal power performance.

Section 4 - Modeling of Complex Rotor Geometry

As discussed in Section 1.2.3, GEC's original intent was to use the ADAMS/AeroDyn codes as the primary design and analysis tools for these complex rotors. However, in the course of the project, substantial challenges were encountered in obtaining reliable results from ADAMS simulations with combined sweep and pre-curve, and as a consequence, GEC shifted the modeling emphasis to FEA-based methods. The following sections provide an overview of both of these modeling approaches, including limitations and issues encountered with each. Specific results from these modeling tools are then presented in subsequent report sections.

4.1 Modeling with ADAMS/AeroDyn

ADAMS (Advanced Dynamics of Mechanical Systems) is a proprietary code from MSC Corp. It is basically a tool to describe the large displacements and rotations of mechanisms, but includes elastic connections and the ability to be linked with user-written routines, such as those describing aerodynamic loading. It was adapted for use with wind turbines by NREL staff in the 1990s and, while it is more demanding in computer time than the FAST code, it can be adapted to any type of configuration, such as a rotor with pre-curved and swept blades.

The ADAMS models of wind turbine blades have traditionally comprised a series of between 10 and 20 parts and elastic connections. Each part and its connection to the next part is regarded as an aerodynamic element and is attributed a chord, length, and aerodynamic twist angle. As the blade moves and deforms, the attached "markers" that represent the aerodynamic chord orientation also deform.

The ADAMS file describing all of the physical details of the wind turbine is complex and it is typical that some kind of preprocessor be used to build up this file. NREL initially developed a code named ADAMS/WT which operated through the ADAMS/view code. More recently NREL has developed a Fortran code which translates an input file for the FAST code and writes out an ADAMS data file. GEC has historically used their own Fortran pre-processor (WTprep) to carry out this step and has thereby been able to incorporate new features as required. For this project, WTprep was further modified to accept pre-curved and swept blades of any extent and to include the additional features needed.

For a straight or nearly straight blade there is little ambiguity about the definition of these quantities and the routines that calculate the aerodynamic loading (the "AeroDyn" routines) have been written with this type of blade in mind. In the current AeroDyn code, the transformations between the blade chord and the plane of rotation (in which the momentum balance is carried out) are simple, and may not be fully valid when the blade is bent through large angles.

Figure 6 shows, schematically, a blade that has both pre-curve and pre-sweep. The coordinate system is consistent with the IEC 61400 design code [3]. The "plane of rotation" is the Y-Z plane.

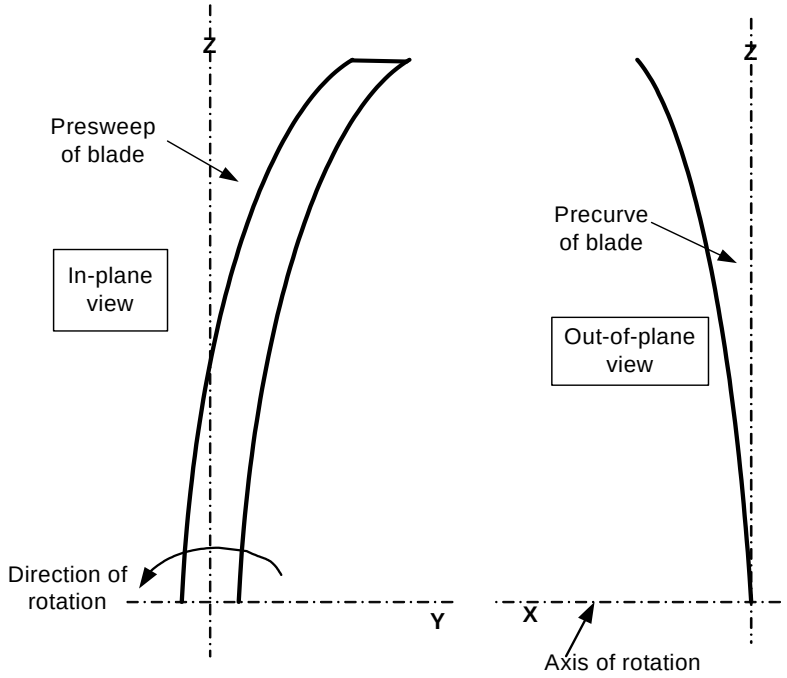

Figure 6. Idealized Blade with Both Pre-Curve and Pre-Sweep

The chord line stretches from the leading to the trailing edge of the airfoil section but there are several possible ways in which the orientation of this line can be defined. It can be considered parallel to the Y axis, as implied by the sketch in Figure 6, or it could be defined as normal to the line generating the curved shape (see Figure 7). Alternatively, it can be defined as normal to a line radial from the X axis (see Figure 7). Because this last definition is aligned with the direction corresponding to the motion of the blade, it was considered the most appropriate for aerodynamic calculations.

In the ADAMS model, one "marker" (a point with its own local coordinates to which forces and connections can be added) is located on each part aligned with the tangent line and is compared with a similarly aligned marker at the blade root in order to measure the physical twist of the blade.

Another marker is added to each part and is aligned with the radial line in order to define a chord that is parallel to tangential motion of the blade part. This marker is also rotated to be aligned with the initial twist or pitch of that portion of the blade. Changes in the pitch angle are then measured by comparison with a similarly aligned marker attached to the root of the blade. These pairs of markers are illustrated in Figure 8.

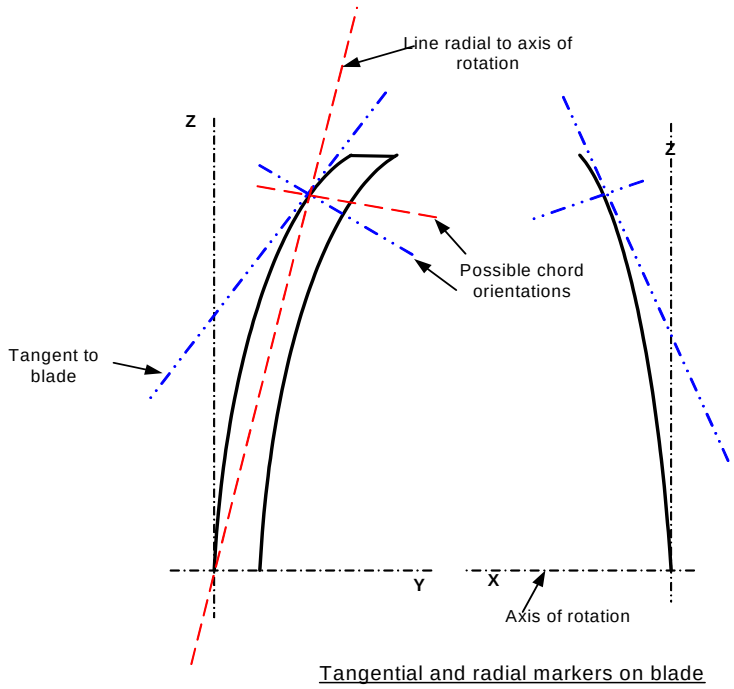

Figure 7. Illustration of Possible Chord Definitions

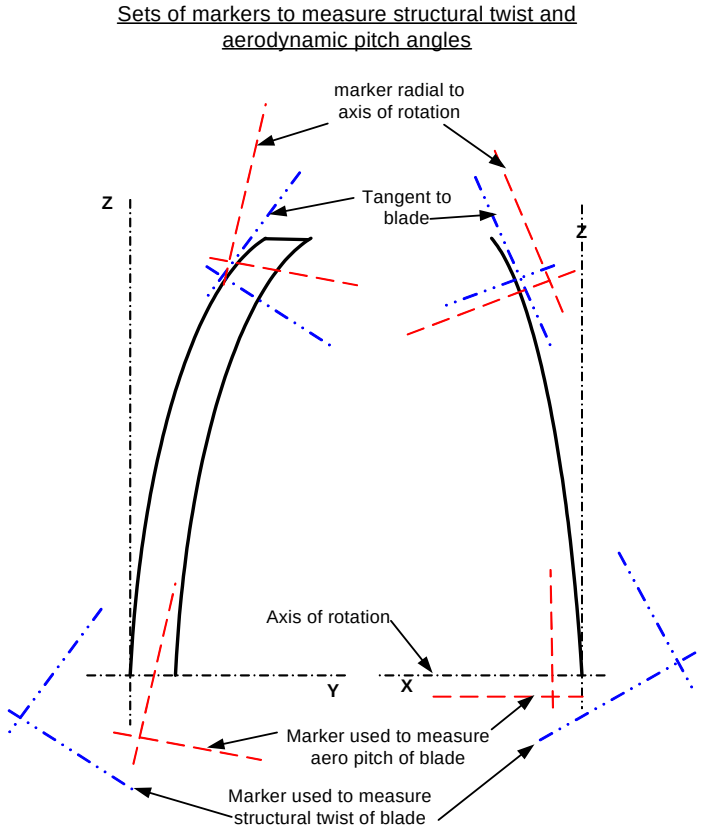

Figure 8. Pairs of Markers to Measure Structural Twist and Aerodynamic Pitch Angles

In the AeroDyn routines, the aerodynamic forces are calculated in the current coordinates of the blade. Those forces are transformed, using only the aerodynamic pitch rotation, into coordinates that are normal and tangential to the plane of rotation and the momentum-balance equations are applied in that plane. This requires that any motion of the blade and the resultant induced velocity and angle of attack also be calculated with respect to the plane of rotation (see Figure 9).

The small-angle approximations in the current AeroDyn code are not valid for a more general case of large pre-curve and sweep, when a more complete transformation between the orientation of the blade element and the plane of rotation should be applied. It was noted during the project that the current AeroDyn routines can lead to spurious motion of the blade normal to the plane of rotation and incorrect angles of attack.

GEC concluded that a comprehensive rewriting of some parts of the AeroDyn routines would be required to apply the appropriate transformations for the general case of large sweep and pre-curve. Such algorithm modifications are beyond the scope of work planned for this project. However, the challenges encountered in this project may prove to be valuable in identifying these limitations, which may then be addressed in future revisions of the AeroDyn routines.

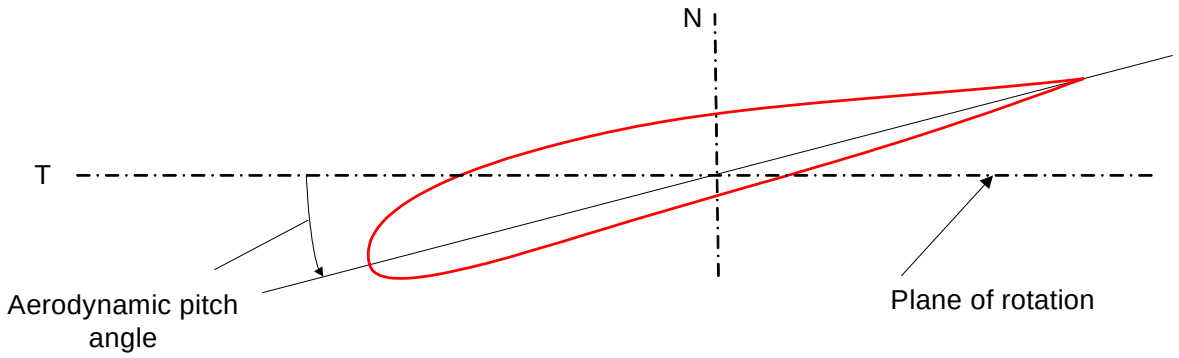

Figure 9. Chord Line and Its Relationship to the Plane of Rotation

4.2 Modeling with SolidWorks/COSMOS

Early in this project, solid models of the AIR-X blade were developed for the purpose of determining mass and stiffness properties as input to the ADAMS models. However, as ongoing challenges were encountered with the ADAMS simulations, GEC re-visited the possibility of using the SolidWorks (solid modeling) and COSMOS (FEA) codes as primary tools in the design and analysis of swept and pre-curved blades.

Because of the multi-dimensional nature of this design problem, GEC sought to develop efficient methods of generating and analyzing blades with complex geometry. Figure 10 illustrates the method used to generate blade geometries in SolidWorks. A series of "sketch planes" were created with the SD2030 airfoil shape. In each plane, the airfoil can be scaled to the desired chord dimension. A series of equations were then used to control the location (X-Y-Z

coordinates) and rotation of the sketch planes, as well as the scaling of the airfoil within each plane. Finally, a solid surface was lofted through the sections defined by the sketch plane to create a solid model of the complete blade.

Once this approach was set up and coded within SolidWorks, complex blade geometries could be rapidly generated. The resulting solid models were then analyzed using the COSMOS FEA code, which runs inside the SolidWorks environment. Figure 11 shows an example of a meshed blade. Both centripetal and aerodynamic loads can be approximated in the COSMOS analyses, which will be discussed in detail in Section 6.0.

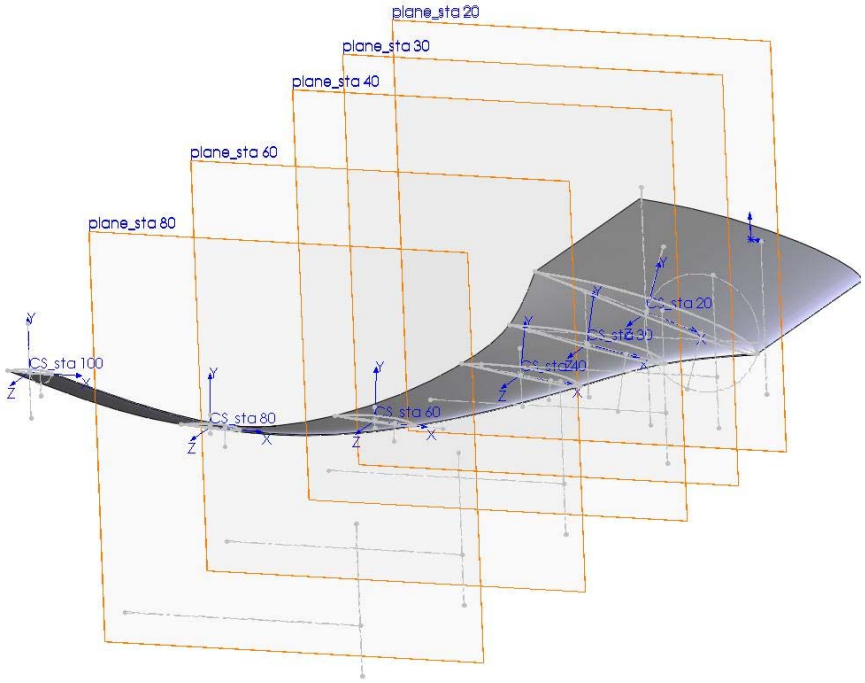

Figure 10. "Sketch Planes" Used in SolidWorks to Derive Complex Blade Shapes

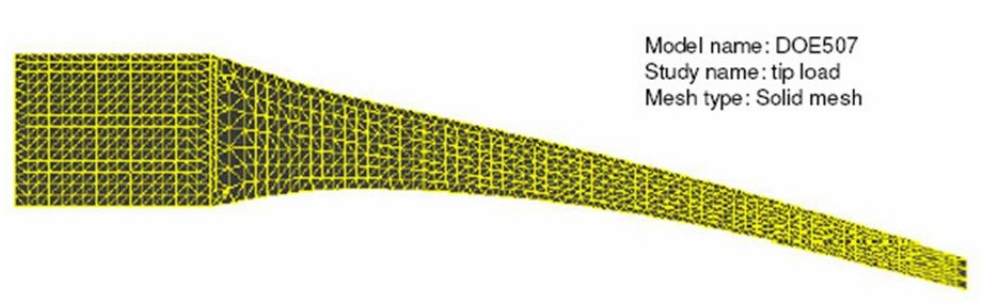

Figure 11. Example COSMOS Mesh of Swept Blade Shape

Section 5 - Alternative Aerodynamic Designs

In initial meetings, GEC and SWWP engineers reviewed the basic aerodynamic and aeroelastic characteristics of the AIR/AIR-X blades. In general, the aerodynamic design (chord and twist distribution) will affect the mass and stiffness distributions of a blade, as well as the aerodynamic loading, and ultimately the aeroelastic response if sweep and pre-curve are added. Because of the interdependent nature of these design variables, it was agreed that alternative aerodynamic designs should be considered in this project.

5.1 Candidate Airfoils

The possibility of using an alternative airfoil in this blade design was considered. Initially, the list of candidates included the six airfoils evaluated by NREL for potential use on small wind turbines [4,5]. However, due to the low Reynolds numbers (Re) that characterize these blades, the list of candidates was reduced to only two: the SD2030 which is used in the current AIR-X blades, and the E387. These foils are depicted in Figure 12.

Figures 13 and 14 show measured aerodynamic characteristics of the airfoils at Reynolds numbers of 100,000 and 200,000, respectively [5]. As seen in Figure 13, at Re = 100,000 the E387 exhibits a substantial rise in drag for angles of attack between 0° and 6°. Reference 5 attributes this to the presence of a laminar separation bubble. At Re = 100,000, the SD2030 drag curve also shows this attribute, but to a much lesser extent than the E387. Inspection of Figure 14 indicates that this characteristic of the drag curves is largely eliminated by Re = 200,000.

Figure 15 shows the approximate Re variation with wind speed for the baseline AIR-X rotor. The data shown in the figure were calculated at the 75% span blade location, based on rotational velocities assuming an operational tip speed ratio of 8.5. Note that although rotational speed decreases in the inner portions of the blade span, chord dimensions increase so that the data of Figure 15 characterize most portions of the AIR-X blade span. As seen in the figure, the baseline AIR-X blade is at Re values below 200,000 over most of its operational range. Because of this, and the strong Re-dependence exhibited by the E387 at very low Re, GEC decided to retain the baseline SD2030 in the further evaluation of alternative aerodynamic designs.

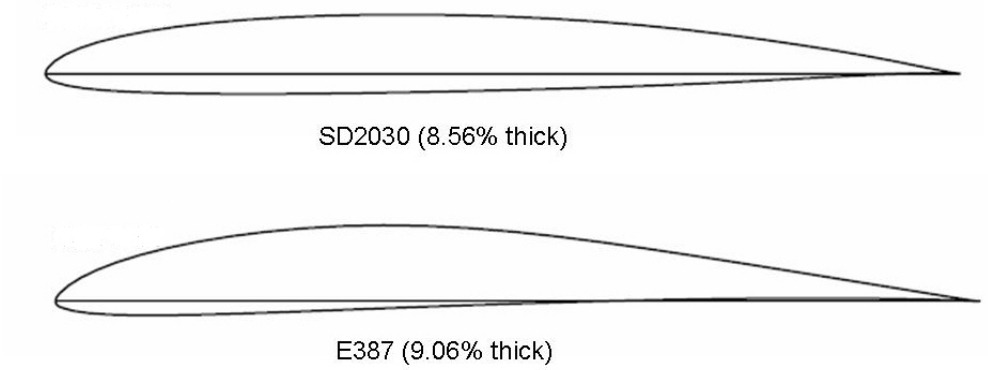

Figure 12. Airfoils Considered for Alternative Aerodynamic Designs

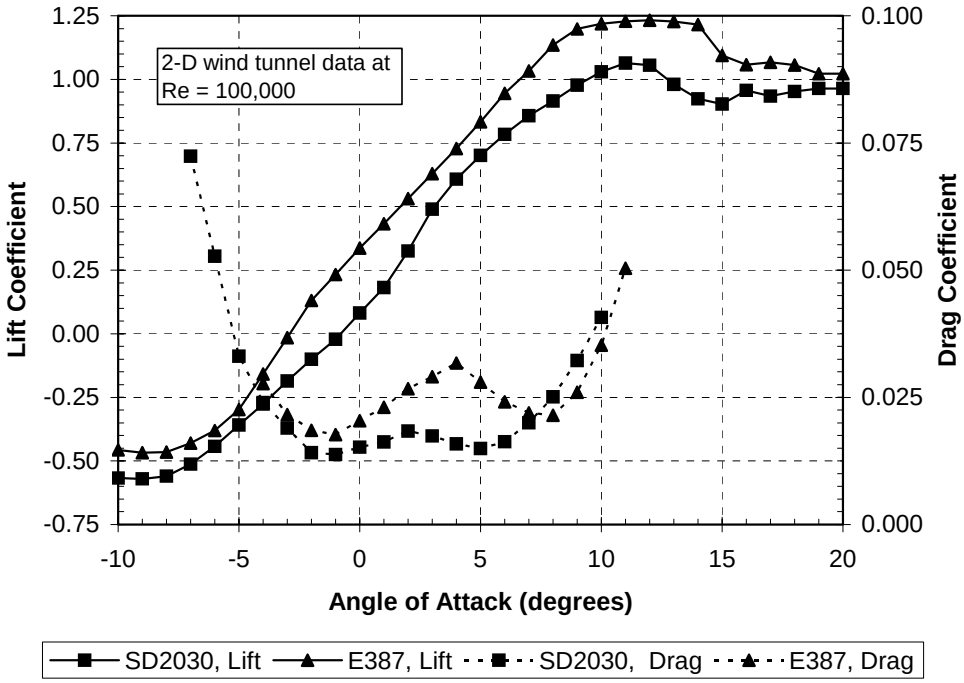

Figure 13. Lift and Drag Curves for Airfoils at Re = 100,000

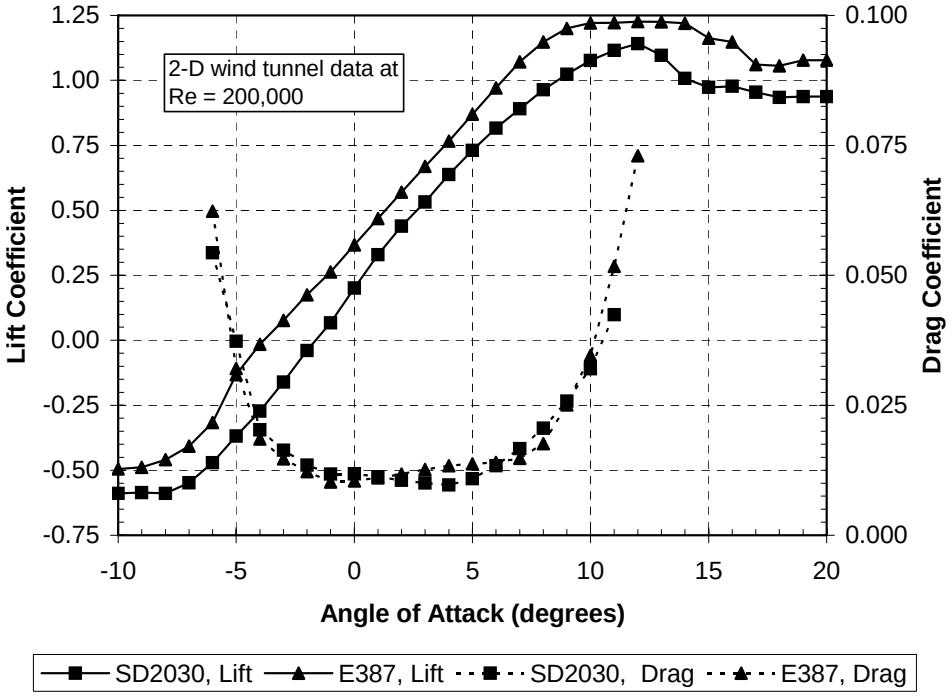

Figure 14. Lift and Drag Curves for Airfoils at Re = 200,000

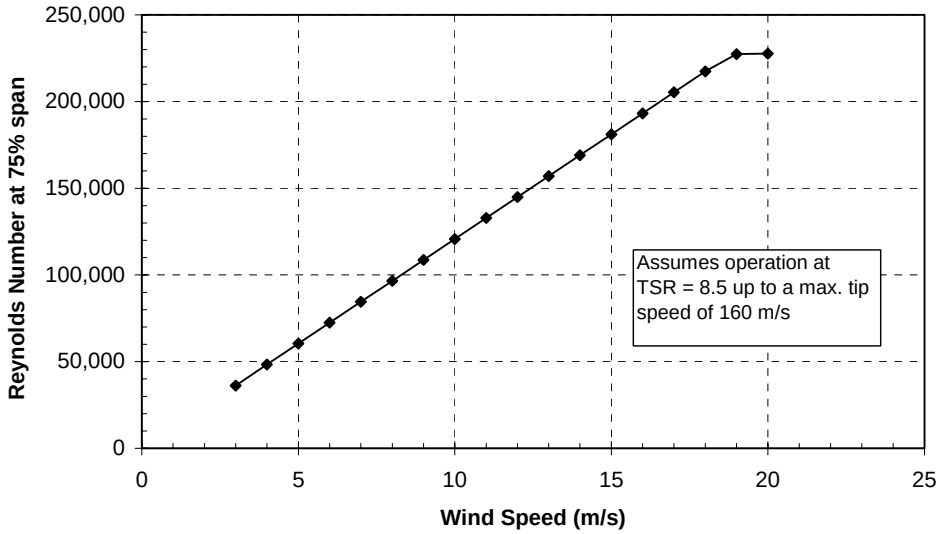

Figure 15. Approximate Re Variation for Baseline AIR-X Blades

Having selected the SD2030, the two-dimensional (wind tunnel) aerodynamic properties were modified to reflect three-dimensional stall-delay effects. The Du-Selig method [6] was used for these adjustments, with the drag correction as proposed by Eggers [7]. Figure 16 shows the resulting curves. As expected, the 3-D adjustments are greatest in the inner blade and the aerodynamic characteristics are approaching their 2-D values by mid-span.

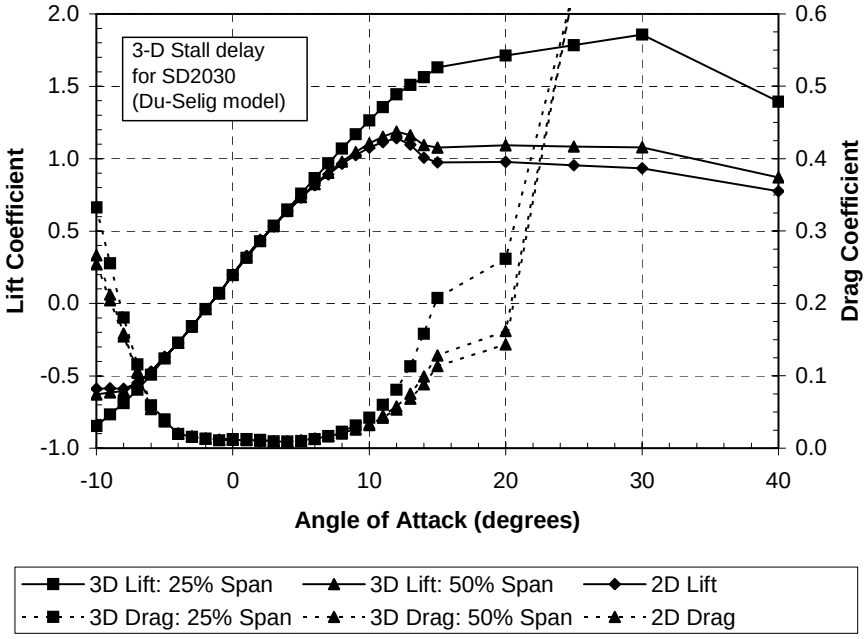

Figure 16. 3-D Adjustments of SD2030 Aerodynamic Properties

5.2 Alternative Planforms

Having selected the SD2030 airfoil, alternative planforms (chord and twist distributions) were investigated. In this process, the PROPID inverse-design code [8] was used to rapidly generate near-optimal aerodynamic designs. Once the blade dimensions were determined, the WT_PERF code was used to evaluate each blade for a range of pitch angles.

The basic methodology for the PROPID designs is described in detail in Reference 9. In general, the designs are driven by two design-specified inputs: The first is the tip speed ratio at peak power coefficient (C_P). This is known as the design tip speed ratio (TSR_D). The second input is the lift coefficient at peak C_P, also know as the design lift coefficient ($C_{L,D}$). TSR_D is specified for the entire rotor, whereas the value of $C_{L,D}$ can be varied at each blade segment. However, because the blades in the current study incorporate only a single airfoil, the design inputs did not include spanwise variation of $C_{L,D}$.

For any given airfoil (or family of foils), peak aerodynamic efficiency is realized when (1) the airfoils are operating near the maximum lift/drag condition, and (2) each rotor segment is extracting the optimal amount of energy from the free-stream wind. In the terminology of blade element momentum (BEM) theory, this latter requirement is met when the "axial induction factor" is near 1/3. This optimal loading condition is closely related to the product of local blade chord and lift coefficient ($C_L \cdot c$). Therefore, the value of $C_{L,D}$ and the resulting chord dimensions for near-optimal performance will vary in an inverse relationship.

Figure 17 shows the variation of SD2030 lift-to-drag (L/D) ratio with lift coefficient for varying Re. A strong Reynolds number dependence is seen, with the magnitude of maximum L/D nearly doubling in the range of Re = 100,000 to 300,000, along with a trend toward lower values of C_L at L/D_{Max}.

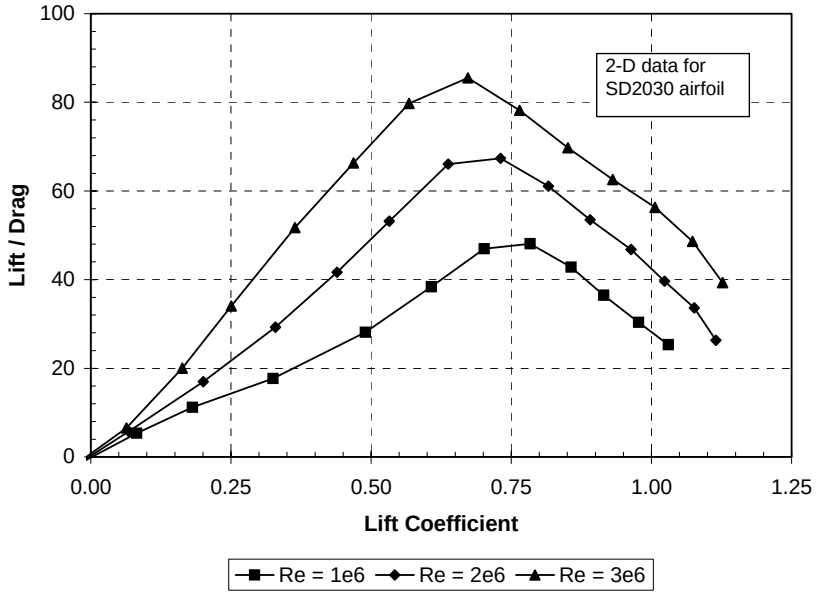

Figure 17. Lift-to-Drag Ratios for SD2030 Airfoil

Based on the trends of Figure 17, alternative blade designs were developed for values of $C_{L,D}$ ranging between 0.6 and 0.8. This parameter sweep was performed for two different values of TSR_D: 7.5 and 8.5. Based on the analysis of these blades, a value of $C_{L,D} = 0.7$ was selected for the subsequent investigations of alternative aerodynamic designs.

Next, a parametric sweep was performed by varying TSR_D between 6.5 and 9.0. Figure 18 summarizes the resulting C_P-TSR curves. While the curves track TSR_D in the expected manner, the variation in peak C_P with TSR_D is quite small.

Figure 19 shows the chord distributions for these blade designs. Inspection of the figure indicates that the chord dimensions increase with decreasing TSR_D. The baseline AIR-X blade (heavy line with diamond symbols) has chord dimensions consistent with a $TSR_D \cong 8.5$.

Figure 20 illustrates the effect of these alternative planforms on operational Reynolds numbers. The figure shows Re strictly increasing with decreasing TSR_D, which indicates that the increased chord dimensions are more than compensating for the reduction in rotational speed at reduced TSR_D.

Based on all of the aerodynamic design trade-offs, a design corresponding to $C_{L,D} = 0.7$ and $TSR_D = 7.5$ was selected as an alternative to the baseline AIR-X planform for evaluation in a complex (swept and curved) geometry. Modeling of the blade with alternative aerodynamic design is presented in Section 6.3. Note, however, that the majority of modeling for complex shapes was done using the baseline AIR-X planform.

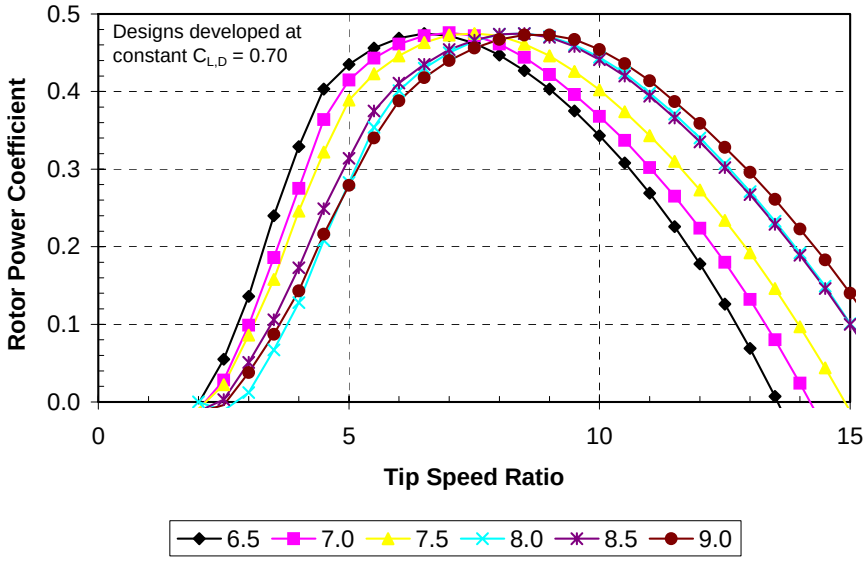

Figure 18. C_P-TSR Curves for Varying Design Tip Speed Ratio

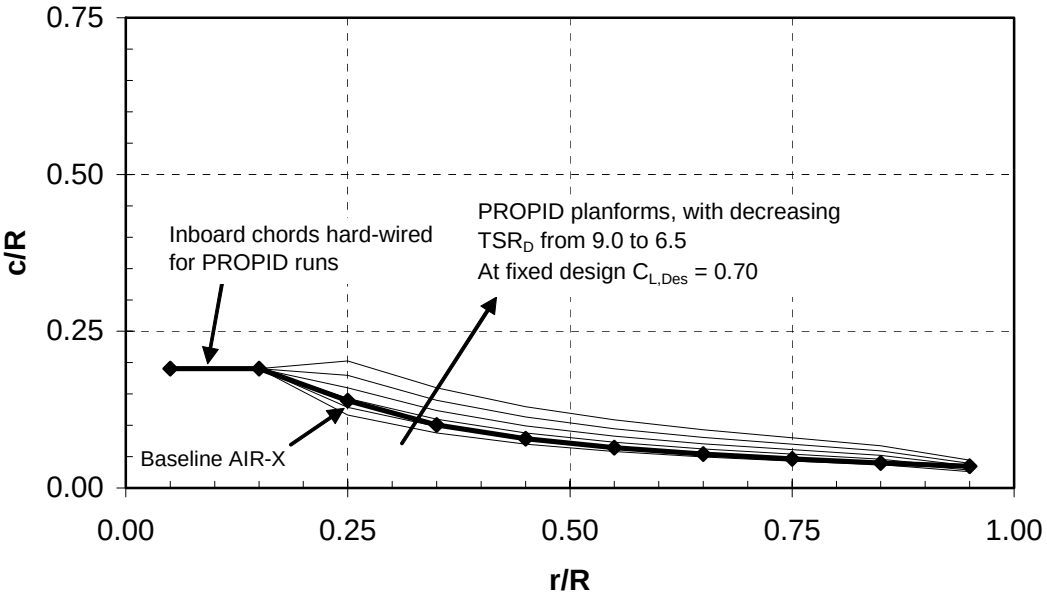

Figure 19. Variation of Planform (Chord Dimensions) with TSR_D

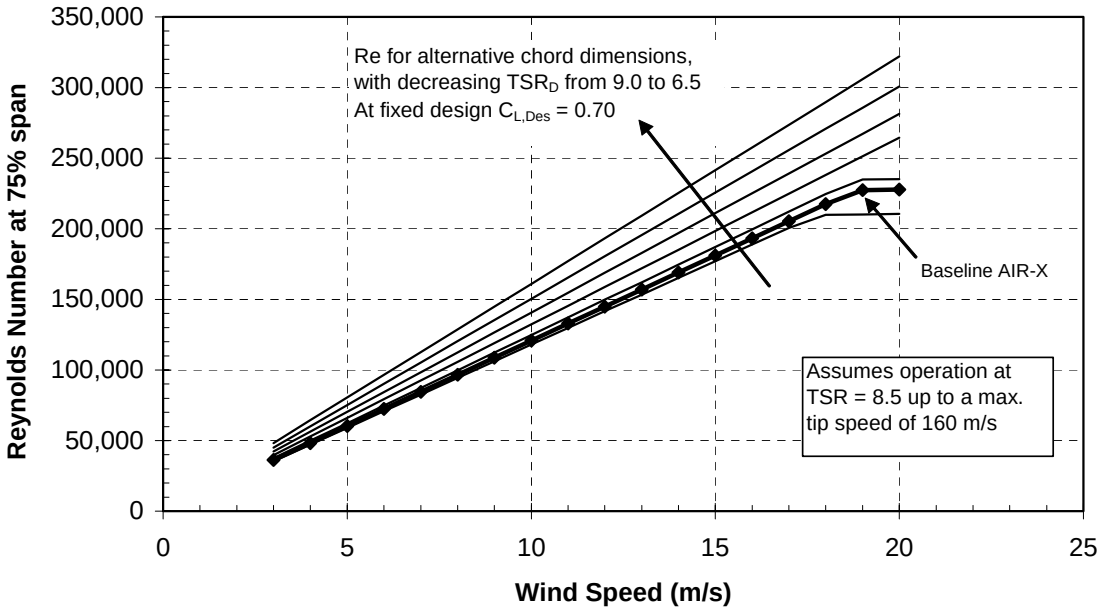

Figure 20. Variation of Reynolds Number with TSR_D

5.3 Blade Structural Modeling

Structural properties of the blade were calculated using the SolidWorks solid-modeling code. Figure 21 shows the results of an "area properties" analysis for the SD2030 airfoil. The mass and stiffness properties for that baseline blade are developed assuming the material properties for Celstran® PP-GF30-20. The basic materials used are:

$E_x = 6.41$ GPa (Eqn. 1)

$G_{xy} = 1.28$ GPa (Eqn. 2)

$\rho = 1120$ kg/m^3 (Eqn. 3)

Since this plastic material includes oriented (fiberglass) short fibers, it is orthotropic ($Ex \neq Ey$). However, because the sections are solid and homogenous, the stiffness properties may be found by a simple multiplication of the material modulus and area moments of inertia. Applying this principle, and using the relationships depicted in Figure 21, yields the following scaling equations:

$\text{Mass (kg/m}^3) \cong 67.8 \cdot c^2$ (Eqn. 4)

$EI_{Flap}\ (\text{N-m}^2) \cong 178 \cdot c^4$ (Eqn. 5)

$EI_{Edge}\ (\text{N-m}^2) \cong 2{,}100 \cdot c^4$ (Eqn. 6)

$GJ\ (\text{N-m}^2) \cong 81 \cdot c^4$ (Eqn. 7)

Equations 4-7 were used in developing the blade stiffness properties for input into ADAMS models. For calculations using finite element analysis (FEA), the material properties in Equations 1-3 were input, along with the 3-dimensional shape, directly into the models.

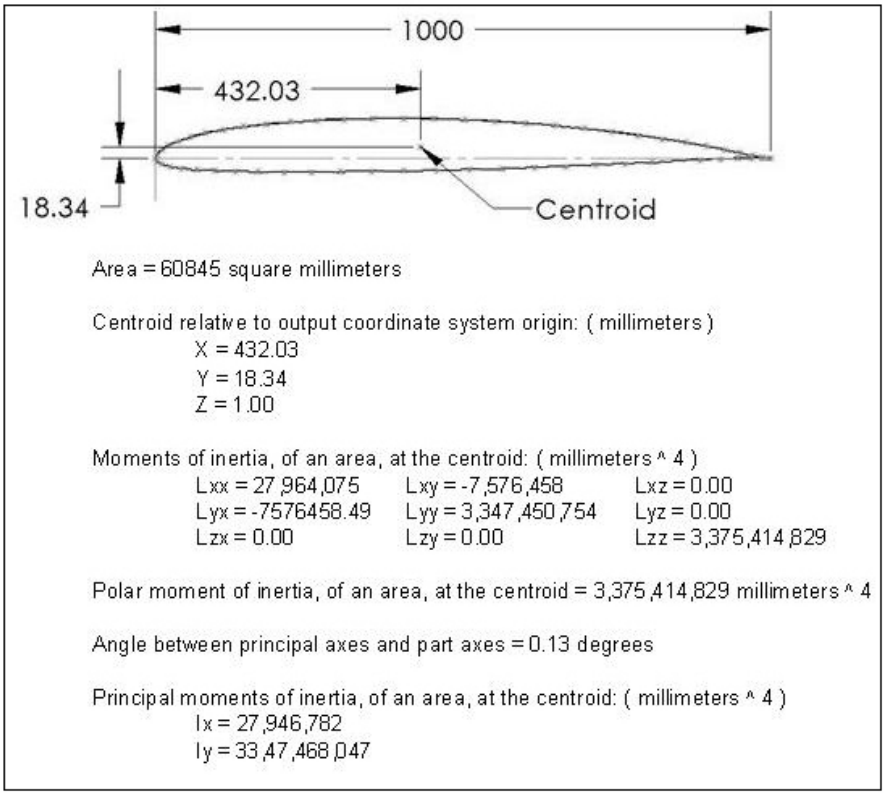

Figure 21. SolidWorks Analysis of Area Properties for SD2020 Airfoil

Section 6 - FEA-Based Modeling of Complex Blade Shapes

6.1 Sweep Variations

To first order, the aerodynamic bend-twist response results entirely from sweep, with negligible dependence of pre-curve. Therefore, the first investigation of complex geometry focused on blade sweep. To identify design sensitivities, two fundamental characteristics were explored: the first was the extent of sweep (with constant sweep curvature) and the second was the shape of the sweep curvature (at constant sweep magnitude). The first parametric variation on sweep is depicted in Figure 22. Planform sweep was defined by the displacement of the tip from the original blade axis, expressed as a percentage of the blade radius (%R). Configurations were evaluated from 0% to 25% sweep in 5% increments. The shape of the sweep curve was defined by a second-order polynomial, hence the curvature was constant over the span for any given design.

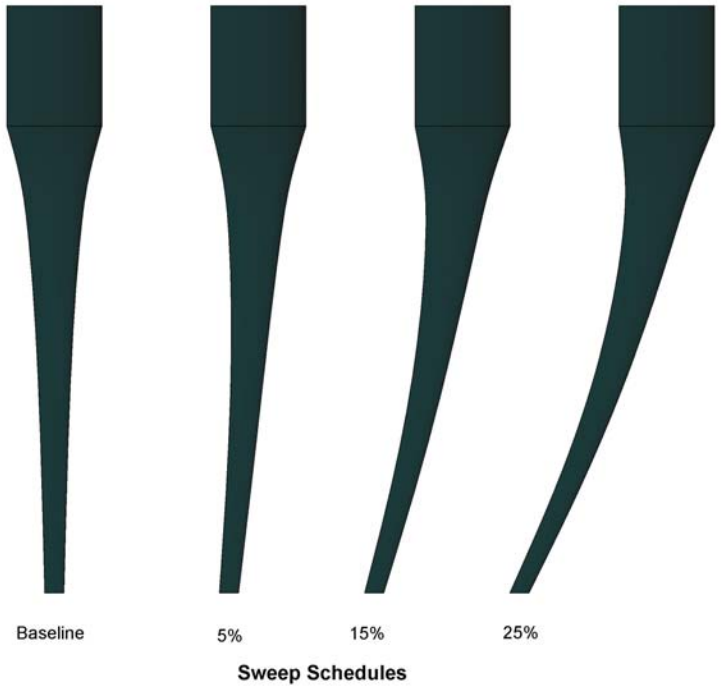

Figure 22. Varying Extent of Planform Sweep

Each configuration was analyzed with the COSMOS FEA code, with a 1 N tip-load applied to mimic the effect of aerodynamic loading. Deflections and tip rotations were measured for each blade under load. Both linear and non-linear FEA simulations were considered. Because the torsional component of the tip-load was largely unaffected by the tip displacement, both simulation methods yielded the same result. Based on this observation, linear FEA analyses were primarily used in evaluating blades with sweep only. The numerical results are summarized in Table 1. There is an apparent flapwise softening of the blade, as the deflections under unit load are increasing with sweep magnitude. The tip rotations similarly increase with

added sweep. To evaluate the relative effectiveness of the sweep in inducing twist, the tip twist results were normalized with respect to tip deflection, with units of degrees per %R of deflection.

These data are presented in graphical form in Figure 23. The deflection curve indicates a marked tendency toward increasing softness of the blade with added sweep. Based on these trends, a sweep of 15% R was identified as efficient in generating twist-response to aerodynamic loads.

Table 1. Effect of Varying Sweep Magnitude (with Fixed Sweep Curvature)

Extent of Sweep (%R)	Tip Deflection		Tip Rot. (Deg.)	Rot. / Deflct. (Deg. / %R)
	(mm)	(%R)		
0%	60.9	10.5%	0.36	0.03
5%	64.5	11.1%	2.29	0.21
10%	67.4	11.6%	4.31	0.37
15%	71.4	12.3%	6.35	0.52
20%	78.0	13.4%	8.67	0.65
25%	85.1	14.7%	11.34	0.77

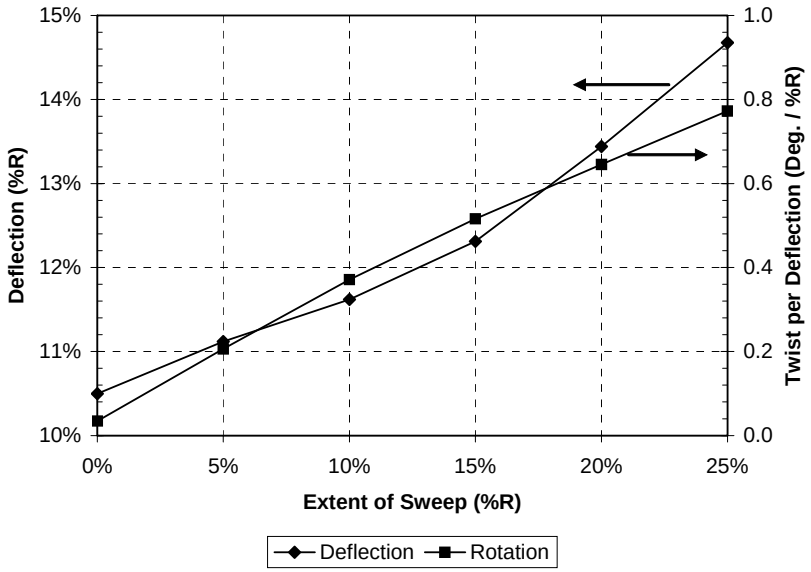

Figure 23. Effect of Varying Sweep Magnitude

Next, the shape of the planform sweep was varied, keeping a constant magnitude (15% R) of sweep at the tip. Sweep distributions were developed using a curve of the general form: $Ax^4+Bx^3+Cx^2+Dx$. By adjusting the coefficients, and normalizing the curve to the desired magnitude of tip sweep, different shapes of sweep were obtained. The results are shown graphically in Figure 24. The "linear" case is essentially kinked near the root with no subsequent curvature. The "Cx^2" case has constant curvature and is the same shape as the 15% R case of Figure 22. In the next two cases, the sweep is concentrated progressively outward on the blade span. The curvature increases linearly with radius for the "Bx^3" case and as the square of radius for the "Ax^4" case.

As before, these configurations were modeled in COSMOS with a unit tip load to evaluate bend-twist response to aerodynamic loading. The results from these cases are given in Table 2. The general trend is one of increasing effectiveness (as measured by tip twist per unit deflection) as the sweep is biased toward the outer span. However, inspection of the loaded FEA models also indicated that the induced twist was concentrated near the tip for these cases. Although outermost blade span has substantial aerodynamic authority, GEC concluded that the constant-curvature (Cx^2) case had the most favorable combination of twist-response magnitude and spanwise distribution.

Table 2. Effect of Varying Sweep Distribution Shape (with Sweep Magnitude = 15%R)

Case	Sweep Curvature	Tip Deflection (mm)	Tip Deflection (%R)	Tip Rot. (Deg.)	Rot. / Deflct. (Deg. / %R)
Dx	Zero	60.9	10.5%	0.36	0.03
Cx^2	Constant	71.4	12.3%	6.35	0.52
Bx^3	Linear with R	74.0	12.8%	7.80	0.61
Ax^4	Increase as R^2	75.9	13.1%	9.06	0.69

Figure 24. Varying Shape of Sweep at Fixed Magnitude (15%R)

6.2 Combined Sweep and Pre-Curve

6.2.1 Centripetal Loading

Achieving a twist-to-stall response to increased rotational speed requires both planform sweep and pre-curve. Based on the trends identified in the sweep-only studies, a sweep configuration of 15% R magnitude and constant curvature was selected as the baseline for investigating the effects of varying pre-curve.

Essentially, the same matrix of design options was investigated for pre-curve as was for sweep: varying magnitude of pre-curve at constant curvature and varying shapes of curvature at fixed magnitude. The matrix of shapes corresponding to varying pre-curve magnitude is entirely analogous to those shown for sweep in Figure 22. The pre-curve shapes evaluated are shown in Figure 25 and are again analogous to those shown for sweep in Figure 24.

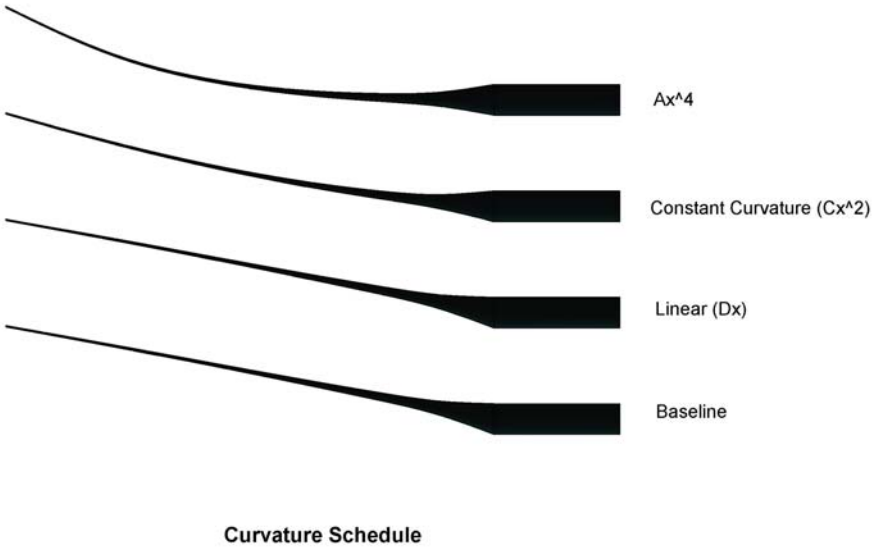

Figure 25. Varying Shape of Pre-Curve at Fixed Magnitude (15%R)

Based on the anticipated AIR-X operational range, FEA models of the swept and pre-curved blades were loaded via centripetal acceleration corresponding to rotor speeds between zero and 2000 rpm. Centripetal loads will increase predictably as the square of the rotation speed. However, the force component that induces deflection and twist (e.g., the mass eccentricity) is a strong function of the displaced blade orientation. As a result, a non-linear, time-varying FEA solution is required to correctly model the structural response to rotation.

Figures 26 and 27 show COSMOS displacement results for a blade with combined sweep and pre-curve at 1000 rpm and 2000 rpm, respectively. Comparing the figures, it is seen that by 1000 rpm, the blade tip is approaching the plane of rotation. As the rotational speed doubles from 1000 to 2000 rpm, the centripetal forces increase by a factor of four. However, because the blade is already bent towards the plane of rotation, the mass eccentricity is much lower than it was at the lower rpm, and the incremental change in tip displacement is modest. This general trend held throughout the cases evaluated, with the blade tip asymptotically approaching the plane of rotation at high rpm values.

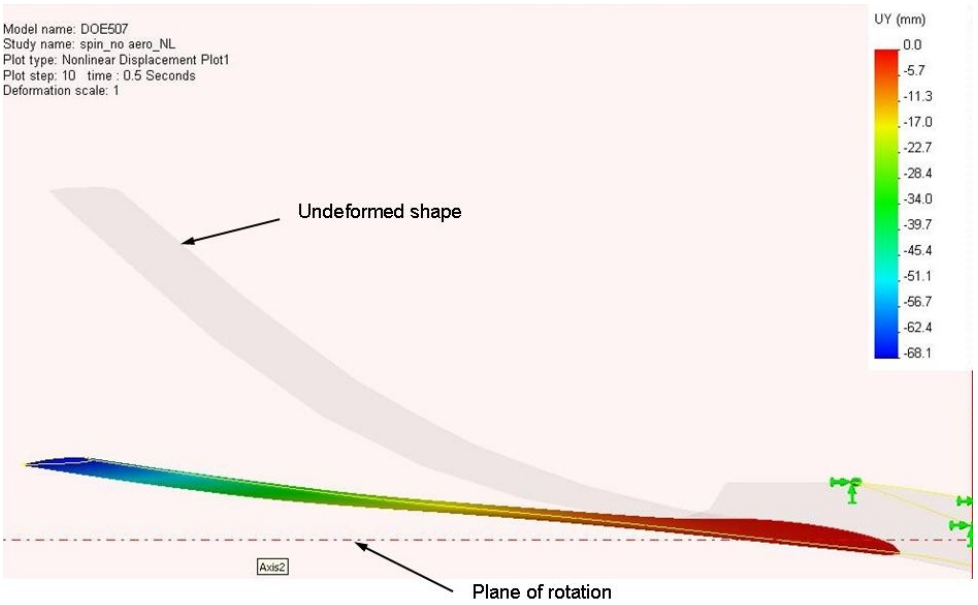

Figure 26. COSMOS Displacement Plot for Combined Sweep & Pre-Curve (1000 rpm)

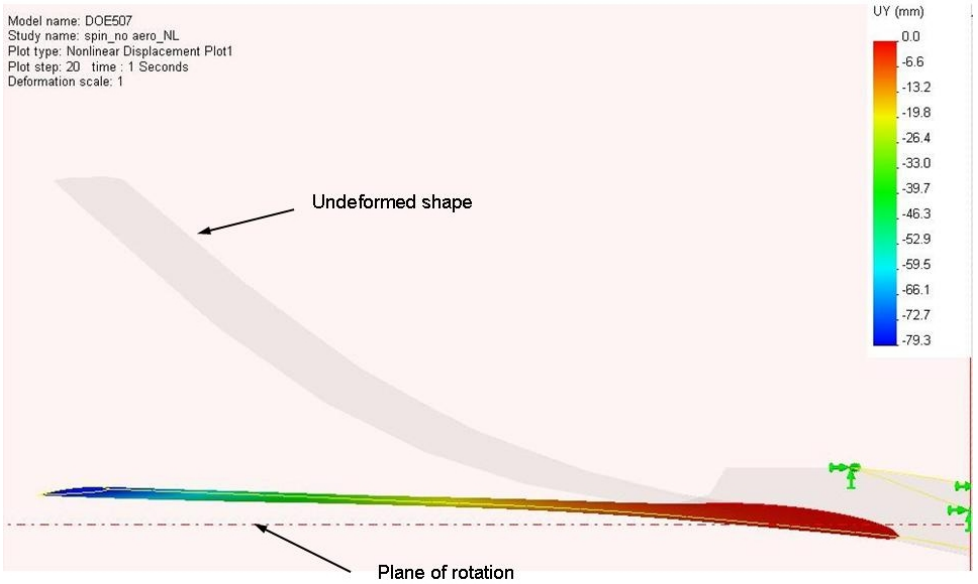

Figure 27. COSMOS Displacement Plot for Combined Sweep & Pre-Curve (2000 rpm)

Figure 28 shows tip rotation at discrete rotational speeds for varying magnitudes of pre-curve, with the shape of the curve fixed at the Cx^2 relationship. To obtain the intended aeroelastic response for the rotor, two conditions are sought: (1) a meaningful amount of twist-response overall, and (2) some slope in the twist-rpm curve at the higher end of the rpm range. For the cases with 15% and greater curvature, the first condition is met. However, for all cases in Figure 28, the twist-rpm slope is small above 1000 rpm. This same general trend was seen for the tip displacements, and the lack of twist-rpm responsiveness at high rpm is correlated with the tip asymptotically approaching the plane of rotation.

Figure 29 shows the effect of varying curvature shapes at a fixed pre-curve magnitude of 15%. The best responsiveness at high rpm is seen for the case with the pre-curve biased toward the outer span (Ax^4 curve). This case was selected for further evaluation with combined centripetal and aerodynamic loading.

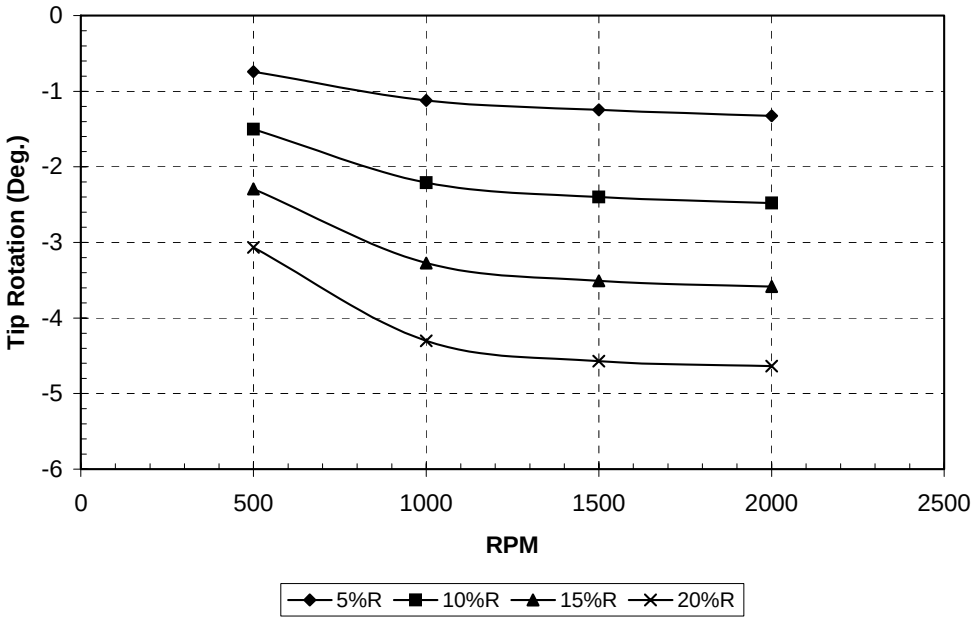

Figure 28. Effect of Varying Pre-Curve Magnitude (Fixed Curvature = Cx^2)

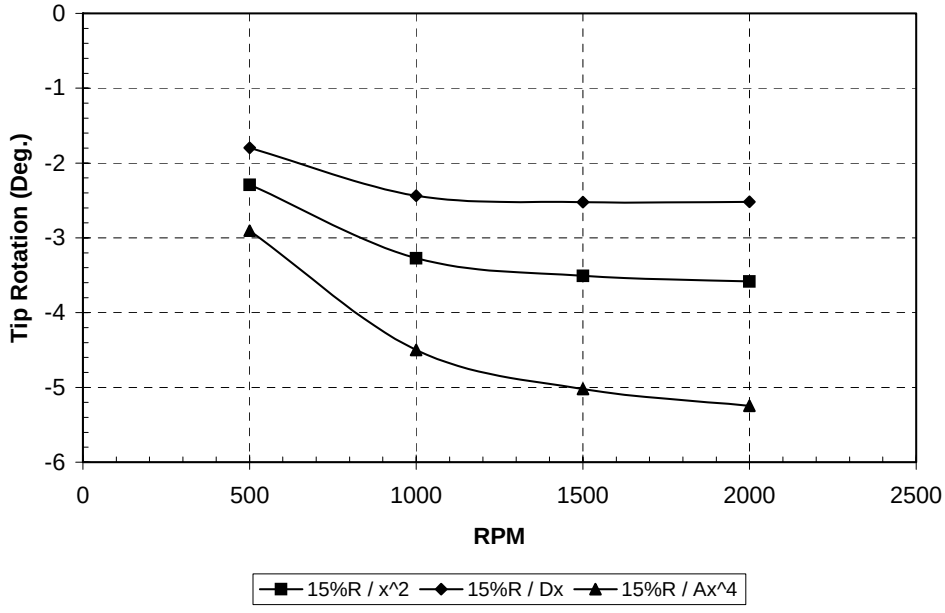

Figure 29. Effect of Varying Pre-Curve Shape (Fixed Magnitude = 15% R)

6.2.2 Combined Centripetal and Aerodynamic Loading

The cases shown in Figures 28 and 29 included only centripetal loading, which tends to force the blade tip upwind toward the plane of rotation. Aerodynamic loads will push the blade in the opposite direction until an equilibrium condition is reached. Reviewing the trends shown in the plots above, it is expected that aerodynamic loads will tend, in general, to push the blades toward a region of greater twist-rpm responsiveness.

However in an actual rotor, the aerodynamic loads themselves are dependent on the blade twist distribution, which changes with both aerodynamic and centripetal loads. Hence, the problem is both non-linear and fully coupled. A simulation code with the complexity of ADAMS is required to correctly model all these dynamic interactions. However, because of the problems encountered in obtaining robust ADAMS simulation results, an attempt was made to use COSMOS FEA modeling to gain insight into the rotor characteristics with combined centripetal and aerodynamic loading.

WT_PERF analyses were used to investigate the aerodynamic condition of the blade in quasi-steady operation. At a tip-speed ratio of 8.5, and operating at peak efficiency, the local blade normal-force coefficients were approximately 0.7. This constant value was used to approximate the blade flapwise bending distribution, which is plotted for the 2000 rpm case in Figure 30.

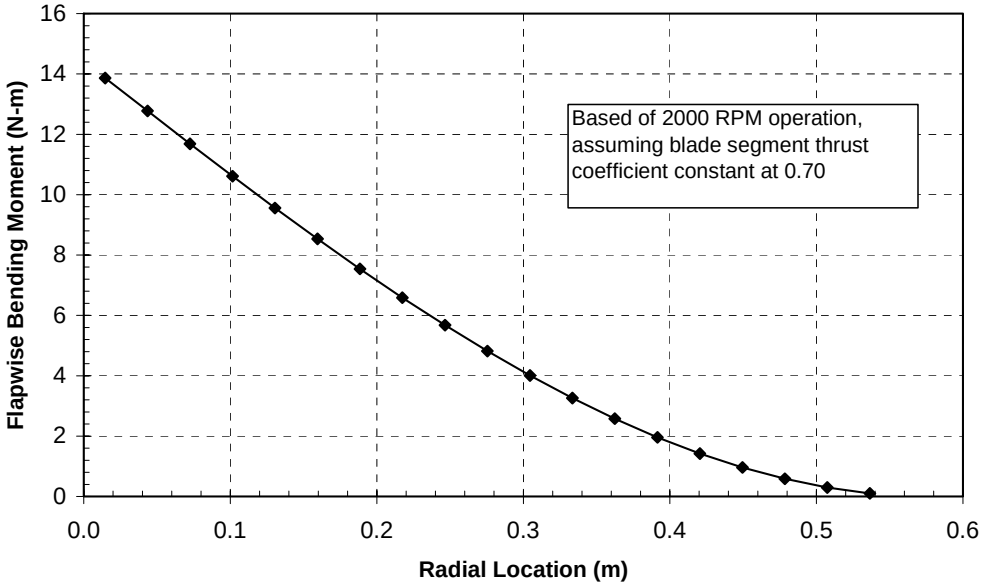

Figure 30. Approximate Bending Load Distribution at 2000 rpm

Various methods were investigated for applying this load distribution to the COSMOS FEA models. Because the combined loading simulation is also non-linear, the aerodynamic loads need to vary both spatially and temporally. Pressure loading was investigated, but proved to be complex to implement. In the end, the most feasible approach seemed to be applying a series of point loads at the airfoil quarter-chord locations, with magnitude varying according to the

spanwise location. This point load distribution was then scaled at each simulation time-step according to the square of the rotational speed.

This approach proved to be both reasonable to apply, and computationally efficient. The results from the COSMOS simulations were somewhat mixed. First, the applied aerodynamic loads had only a modest effect in pushing the blade back away from the plane of rotation, indicating that for this configuration the centripetal loading was dominant. However, the tip rotations seen for this case did not follow the expected trend. Specifically, the addition of the applied loads tended to reduce the tip displacement (as expected), but increase the tip rotation (counter to expectations). Numerous modeling approaches were tried to approximate the aerodynamic loading; however, no method was identified as having the correct balance of modeling simplicity and fidelity.

GEC has done a preliminary investigation of the "FloWorks" computational fluid dynamics (CFD) code which runs in the SolidWorks environment. With that code, CFD simulations can be used to calculate aerodynamic forces, which can then be transferred directly to a COSMOS FEA model. While this appears to be a powerful method for modeling a particular rotor operational point in great detail, the use of such a modeling approach was beyond the feasible scope of work for the present study.

6.3 Additional Parametric Variations of Design Parameters

Following the analyses above, GEC evaluated additional parametric variations on the swept-curved blade. These included the following:

- Changing the assumed material properties for the baseline blade shape:
  - Doubling the extensional stiffness of the material (E_X) while leaving the torsional stiffness (G_{XY}) unchanged.
  - Doubling both E_X and G_{XY}.
  - Leaving the baseline stiffness unchanged, but decreasing mass density by half.
- Modifying the planform (chord and twist) keeping the rotor diameter unchanged:
  - Using the alternative aerodynamic design as discussed in Section 5.2.
  - Resulting planform had chord dimensions on the order of 25% to 30% greater than the baseline AIR-X blade.
- Scaling-up the rotor to larger diameters, allowing chord dimensions to grow in proportion to blade length (rotor diameters two times and four times baseline, with assumed rpm schedule adjusted proportionally).

Each of these configurations was modeled with centripetal loading only. Figure 31 presents the results for assumed modifications to the blade stiffness and mass density properties. All three of the modifications modeled (increased stiffness and decreased mass density) exhibited the same result, which was a very slight increase in twist-rpm responsiveness approaching 2000 rpm.

Figure 32 shows the results for modified blade and rotor geometry. For the alternative planform, almost no change was seen in the response to centripetal loading. For the cases with two times

and four times the baseline rotor diameter, the slope of the twist-rpm curve became increasingly steep with larger diameter. This trend was expected, as it is recognized that centripetal loading becomes less prominent as rotor size is increased. In these cases where the rotor geometry was modified, the aerodynamic forces under operation, and hence the final balance between centripetal and aero loads, would also be different from the baseline configuration. However, because a method for robust modeling of combined centripetal and aero loading was not identified during this study, the end result from these parametric variations is uncertain. The best that can be said from the present work is that material properties and rotor scale can be used to alter the twist-rpm responsiveness, and so could in theory be used to tailor a design to achieve the desired aeroelastic response.

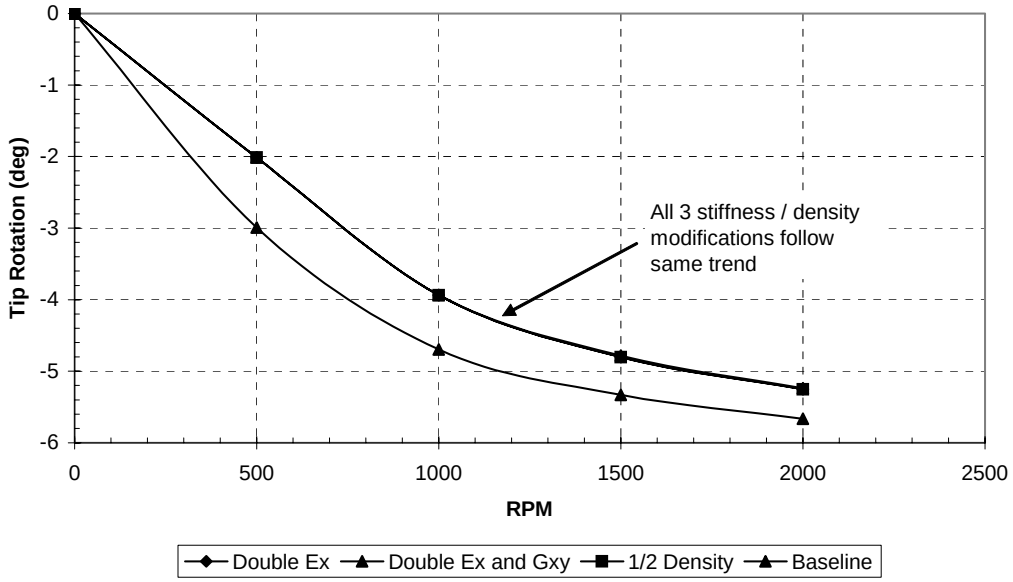

Figure 31. Modifications to Blade Stiffness and Mass Properties (Centripetal Loading Only)

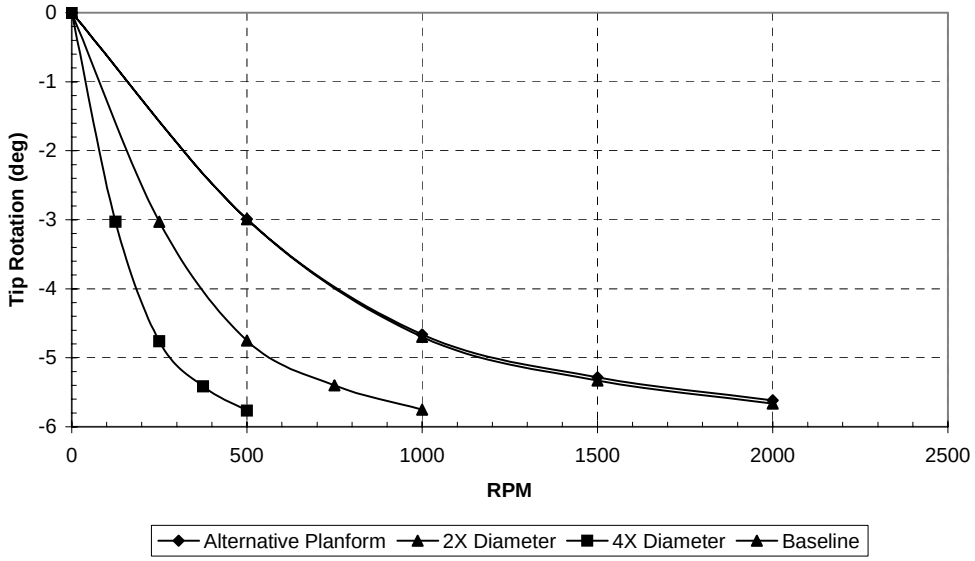

Figure 32. Modifications to Blade Planform and Rotor Diameter (Centripetal Loading Only)

Section 7 - ADAMS Modeling of Complex Blade Shapes

ADAMS modeling was performed for a blade with 15% R sweep (Cx^2 shape) and 15% R pre-curve (Ax^4). Although methods were developed to address some of the issues described in Section 4.1, the ADAMS simulation results still exhibit some anomalous trends.

Figure 33 shows tip rotations under centripetal loading, as predicted by both the COSMOS and ADAMS simulations. As seen in the figure, the comparisons are quite good. Although there are slight deviations between the models, for both codes the tip displacements asymptotically approach the plane of rotation at high values of rpm.

Figure 34 shows tip rotations for the same cases. Consistent with the trends presented in the previous sections, the incremental change in tip rotation decreases with rpm for the COSMOS results. The ADAMS predictions are opposite, with relatively small amounts of twist at the lower-end of the rpm range, and increasing twist-rpm response at high rotational speeds. This ADAMS trend is counter-intuitive because, as the blade is spun towards the plane of rotation, the eccentricities that induce twist are expected to diminish.

ADAMS simulations were also performed for this blade with combined aerodynamic and centripetal loading. However because the tip rotations exhibited this unexpected behavior, the reliability of the combined loading simulation results is considered questionable. Substantial effort was expended during this project in an effort to understand the ADAMS simulation results and reconcile/eliminate any anomalous trends. Unfortunately, these issues were not resolved to GEC's satisfaction during the course of this study.

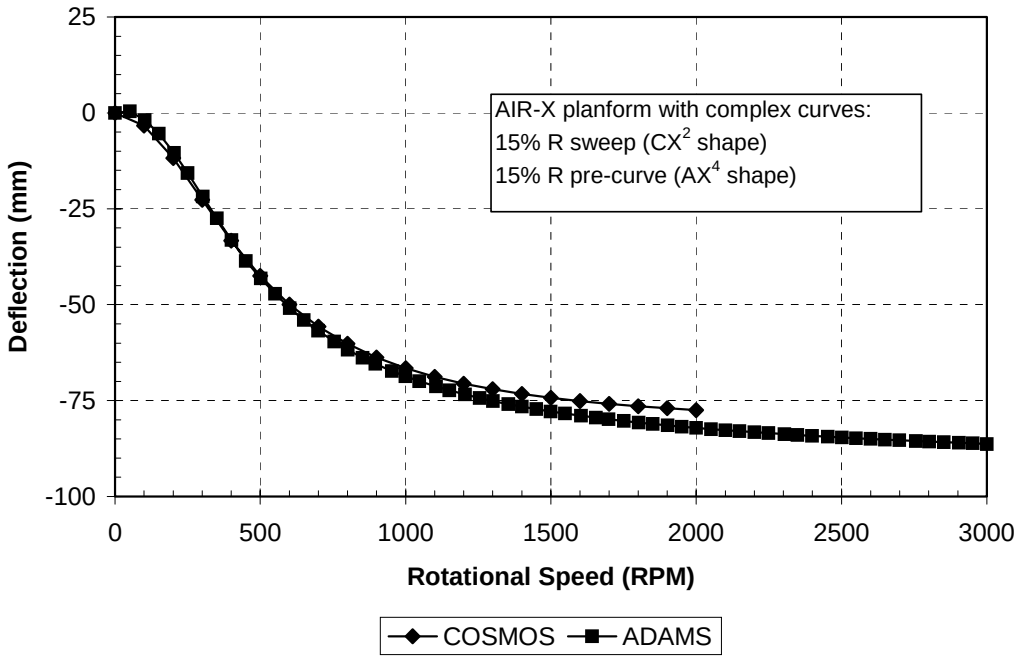

Figure 33. Tip Displacements for Swept-Curved Blade Under Centripetal Loading

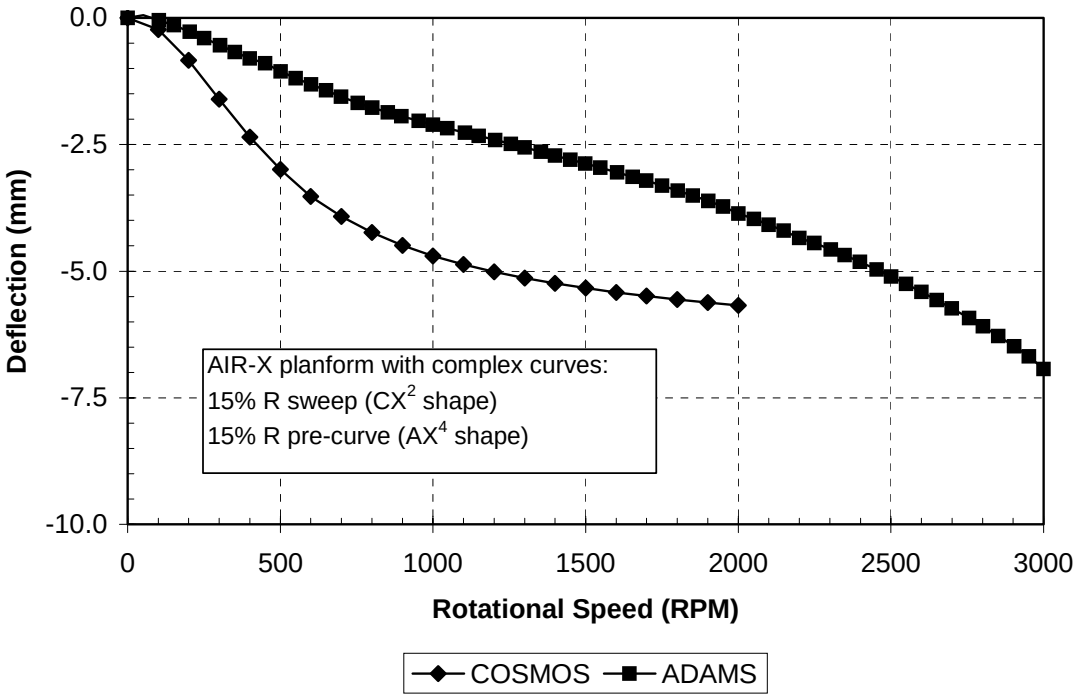

Figure 34. Tip Rotations for Swept-Curved Blade Under Centripetal Loading

Section 8 - Summary

8.1 Conclusions

A novel computational and modeling approach has been developed to evaluate small wind turbine blades with complex geometric shapes. This tool set was used to investigate the potential for aeroelastic tailoring with combined planform sweep and pre-curve. An extensive matrix of design variables was investigated, including:

- Aerodynamic design
  - Airfoils
  - Chord and twist distribution
- Sweep
  - Magnitude
  - Shape of sweep distribution
- Pre-curve
  - Magnitude
  - Shape of pre-curve distribution
- Material stiffness
- Rotor diameter

COSMOS FEA modeling with tip-loads and centripetal acceleration resulted in substantial insights into the structural response of these blades. The trends were used to identify geometries and rotor configurations that showed the greatest promise for achieving beneficial aeroelastic response.

To fully evaluate the aeroelastic behavior of these rotors, the fully coupled interactions between aerodynamic forces, centripetal forces, rotor speed, and blade twist-response need to be accurately modeled. Ideally, this would be done in an aeroelastic simulation code such as ADAMS. Although extensive effort was made to perform such modeling during this project, the final results were not satisfactory. Some observations and conclusions from this modeling effort include the following:

- For such a small and complex rotor, the ADAMS simulations are sensitive to many parameters:
  - The time-step must be kept very small to correctly calculate accelerations and centripetal forces, and
  - Measurement and tracking of blade displacements, aerodynamic, and structural twist must be done carefully.
- Approximations in the current AeroDyn routines are not valid for the large angles and displacements associated with this combined sweep and pre-curve rotor concept.
- The AIR-X blade is very flexible in torsion, which complicated this modeling effort.
- Because of the high centripetal loading, small eccentricities/offsets in the ADAMS beam-elements (used to approximate blade structure) can have large effects in predicted response.

- Both structural response and aerodynamic loading are non-linear. There may be instabilities and bifurcations such that the equilibrium point under operating conditions may be dependent on the order of loading.

With applied tip loads and non-linear analyses with centripetal loading, the results from COSMOS FEA modeling consistently followed intuitive trends. However, when GEC attempted to approximate the combined effects of aerodynamic and centripetal loading, the results were less satisfactory. Because the modeling of centripetal effects requires a non-linear solution, then the applied loading also needs to vary spatially and temporally. GEC made numerous attempts to correctly approximate the combined loading, without complete success.

During the COSMOS FEA modeling efforts. GEC noticed a moderately strong sensitivity of predicted twist angles to the chord-wise location of the applied loads. This is expected, as the load application point will affect the eccentricities that induce twist. However, this also points out a difficulty for modeling of this rotor concept, in that the center of aerodynamic pressure will change with angle of attack, particularly when the local airfoils stall.

8.2 Recommendations for Future Work

GEC has investigated the possibility of combining CFD and FEA modeling in the SolidWorks environment. This approach appears to be computationally feasible and would likely give reliable results for specific operating points. However, for rotor design and analytical evaluation, this approach is not expected to be a satisfactory replacement for aeroelastic simulation.

Although substantial progress in the aeroelastic simulations was made during the course of this project, the effort fell short of achieving entirely reliable results. The large angles and displacements for this rotor concept exceed the approximations in the current AeroDyn routines and, in general, the technology under consideration will be very sensitive to any errors/offsets in the locations of blade loading and beam-connectivity.

The COSMOS FEA modeling of centripetal loading was computationally efficient. The results were deemed to be reliable and provided substantial insight into how the twist-rpm response can be tailored by blade shape, material properties, and rotor scale.

Overall, both the design space and modeling complexity for this technology are extensive. The COSMOS FEA modeling was demonstrated as an efficient tool for narrowing the design space, but fell short of analytically demonstrating the intended aeroelastic response of the rotor. Because of the relatively small scale for which this technology is intended, the most reliable and cost-effective approach may be to gain as much guidance as practical from this type of modeling, then establish the actual aeroelastic response via operational testing of prototype rotors.

Section 9 - References

1. Malcolm, D.J.; Hansen, A.C. *WindPACT Turbine Rotor Design Study: June 2000–June 2002*. 82 pp.; NICH Report No. SR-500-32495. National Renewable Energy Laboratory. August 2002.

2. Zuteck, M. *Adaptive Blade Concept Assessment: Curved Planform Induced Twist Investigation.* SAND2002-2996. Albuquerque, NM: Sandia National Laboratories. October 2002.

3. International Electrotechnical Commission. *IEC 61400-1: Wind turbine generator systems – Part 1: Safety Requirements*, 2nd Edition. International Standard 1400-1. 1999.

4. Somers, D.M, Maughmer, M.D. *Theoretical Aerodynamic Analyses of Six Airfoils for Use on Small Wind Turbines: July 2002-October 2002.* 90 pp.; NREL/SR-500-33295. National Renewable Energy Laboratory. June 2003.

5. Selig, M.S., McGranahan, B. *Wind Tunnel Aerodynamic Tests of Six Airfoils for Use on Small Wind Turbines. October 2002-January 2003.* 133 pp.; NREL/SR-500-34515. National Renewable Energy Laboratory. May 2004.

6. Du, Zhaohui, Selig, M.S. "A 3-D Stall-Delay Model for Horizontal Axis Wind Turbine Performance Prediction." AIAA-98-0021. *A Collection of the 1998 ASME Wind Energy Symposium Technical Papers presented at the 36th AIAA Aerospace Sciences Meeting and Exhibit.* Reno, NV. January 1998.

7. Eggers Jr., A.J, Chaney, K., Digumarthi, R. "An Assessment of Approximate Modeling of Aerodynamic Loads on the UAE Rotor." AIAA-2003-0868. *A Collection of the 2003 ASME Wind Energy Symposium Technical Papers Presented at the 41st AIAA Aerospace Sciences Meeting and Exhibit.* Reno, NV. January 2003.

8. Selig, M.S.; Tangler, J.L. "A Multipoint Inverse Design Method for Horizontal Axis Wind Turbines." Presented at the AWEA Windpower '94 Conference. NREL/CP-500-16336. National Renewable Energy Laboratory. 1994.

9. Griffin, D.G. *NREL Advanced Research Turbine (ART) Aerodynamic Design of ART-2B Rotor Blades.* NREL/SR-500-28473. National Renewable Energy Laboratory. August 2000.